Fe-TiO_2/AC and Co-TiO_2/AC composites: novel photocatalysts prepared from waste streams for an efficient removal and photocatalytic degradation of Cibacron Yellow F-4G dye.

Roberto Machado Garcia [a], Robert Carleer [b], Maria Arada Pérez [a], Jeamichel Puente Torres [c], Ying Gu[d], Pieter Samyn [b], Jan Yperman [b*]

[a] Department of Chemistry, Universidad de Oriente, Patricio Lumumba s/n, CU-90 100 Santiago de Cuba, Cuba. robertomg@uo.edu.cu, mayarada@uo.edu.cu

[b] Research group of Analytical and Circular Chemistry, University Hasselt, Agoralaan, Gebouw D, BE-3590 Diepenbeek, Belgium. jan.yperman@uhasselt.be, robert.carleer@uhasselt.be, pieter.samyn@uhasselt.be

[c] Faculty of Electrical Engineering, Universidad de Oriente, CU-90-100 Santiago de Cuba, Cuba. jeamichelp@gmail.com

[d] Zhejiang Ocean University, Zhoushan 316022, China. guying@hust.edu.cn

1. *pH at the point of zero charge (pH_{PZC})*

In brief, 50 mg of sample were mixed in every bottle with 50 mL of 0.01 M NaCl solutions at various (2–10) initial pH (pH_i) during 24 h in a shaking bath. Afterwards, the pH of the solution (pH_f) was determined. The final (pH_f) and initial (pH_i) pH difference ($\Delta pH = pH_f - pH_i$) was calculated and plotted versus pHi. The pH_{PZC} of the adsorbent is found where the resulting curve intersects the value of $\Delta pH = 0$.

2. *Batch equilibrium studies*

In brief, 25 mL of synthetic CYF-4G dye solution with an initial pH=2 and different concentrations (from 50 to 350 mg/L) was added to each flask with 0.03 g of adsorbent/photocatalyst at 25°C and during 24 h in a shaking bath. After the adsorption, the dye solution was filtered using a 14 A filter paper. The dye concentration of each sample before and after adsorption was measured using a Biochrom Ultrospec 9000 UV-VIS spectrophotometer at $\lambda max = 420$ nm

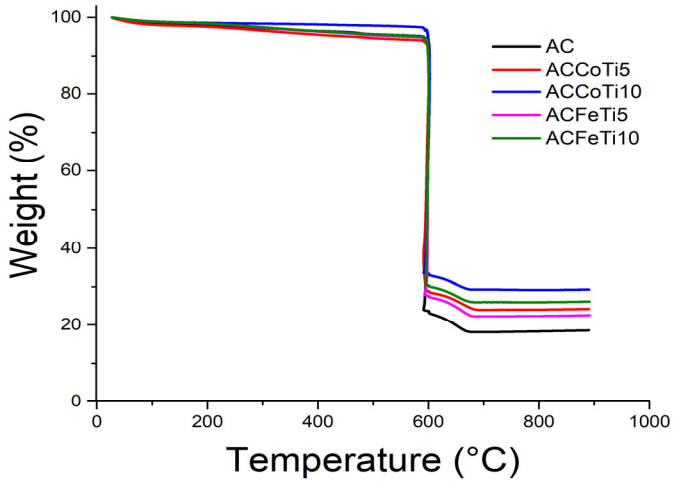

Figure S1. TG curves of AC, ACCoTi5, ACCoTi10, ACFeTi5 and ACFeTi10.

Table S1. Proximate analysis of AC, Fe-TiO_2/AC and Co-TiO_2/AC composites.

	Proximate analysis (wt. %)*					
Samples	MC	VM	FC	Ash 900 °C	CO_2 mass loss	$CaCO_3$ content
AC	1.56	2.03	74.48	17.19	4.74	10.77
ACFeTi5	1.37	3.62	68.04	22.55	4.42	10.05
ACFeTi10	1.32	3.45	64.25	26.72	4.26	9.679
ACCoTi5	1.82	4.82	64.57	24.15	4.64	10.54
ACCoTi10	0.98	2.53	63.01	29.30	4.18	9.50

MC is moisture content, VM is volatile matter, FC is fixed carbon, *error on proximate analysis is 5 %.

Table S2. Elemental analysis

	Elemental analysis (%)						**Molar Ratio**	
Samples	C	H	N	S	Ash	O*	H/C	O/C
AC	73.80	1.04	0.75	<DL	17.19	7.22	0.014	0.098
ACFeTi5	67.20	0.74	0.61	<DL	22.55	8.90	0.011	0.132
ACFeTi10	62.36	0.81	0.63	<DL	26.72	9.48	0.012	0.152
ACCoTi5	65.90	0.72	0.59	<DL	24.25	8.54	0.011	0.129
ACCoTi10	59.80	0.58	0.66	<DL	29.3	9.66	0.010	0.162

*Calculated by difference. O%= 100% - (C%+N%+H%+S%+ash%); b on dry basis. DL= detection limit.

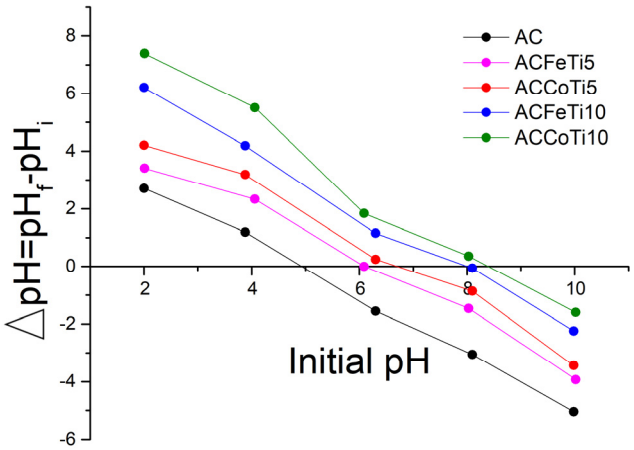

Figure S2. Point of zero charge measurements for AC, ACCoTi5, ACCoTi10, ACFeTi5 and ACFeTi10.

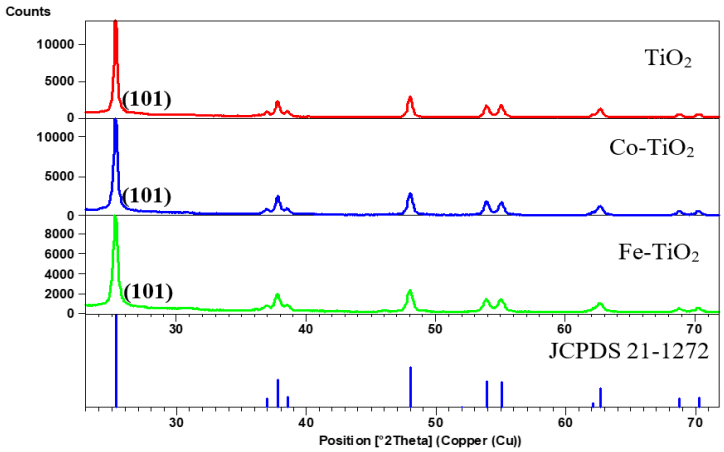

Figure S3. X-ray diffraction patterns of TiO_2, 0.5 wt.% Co-doped and 1 wt.% Fe-doped TiO_2.

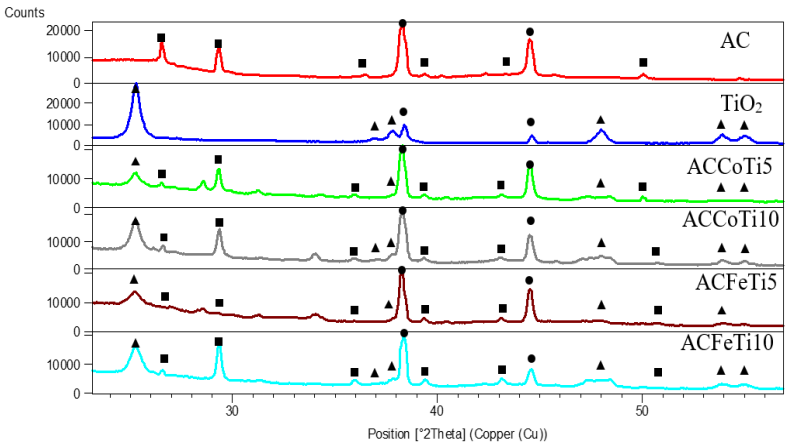

Figure S4. X-ray diffraction patterns of AC, TiO_2, ACCoTi5, ACCoTi10, ACFeTi5 and ACFeTi10. Peak labelling corresponds to the following: ■ AC; ▲Anatase and ●Al peaks (from sample holder).

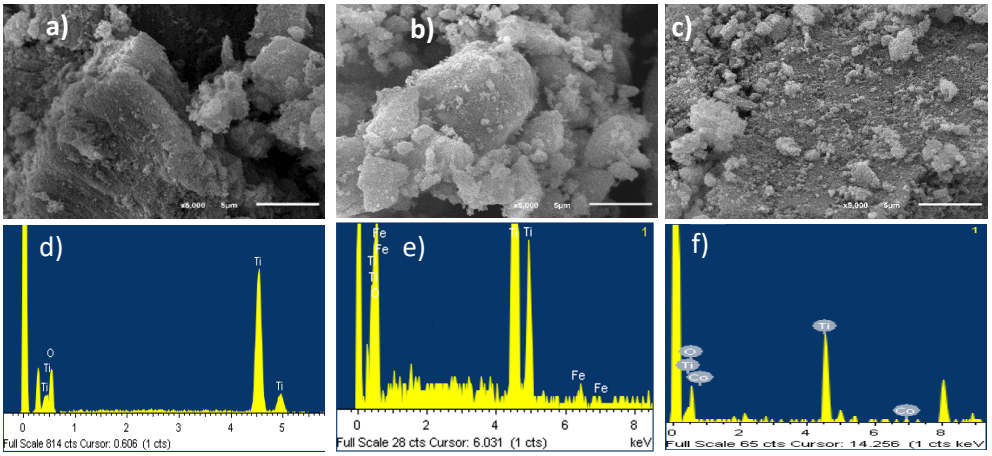

Figure S5. Scanning electron microscopy images of: a) TiO_2, b) Fe-TiO_2 and (c) Co-TiO_2 and EDS spectra of d) TiO_2, e) Fe-TiO_2 and f) Co-TiO_2.

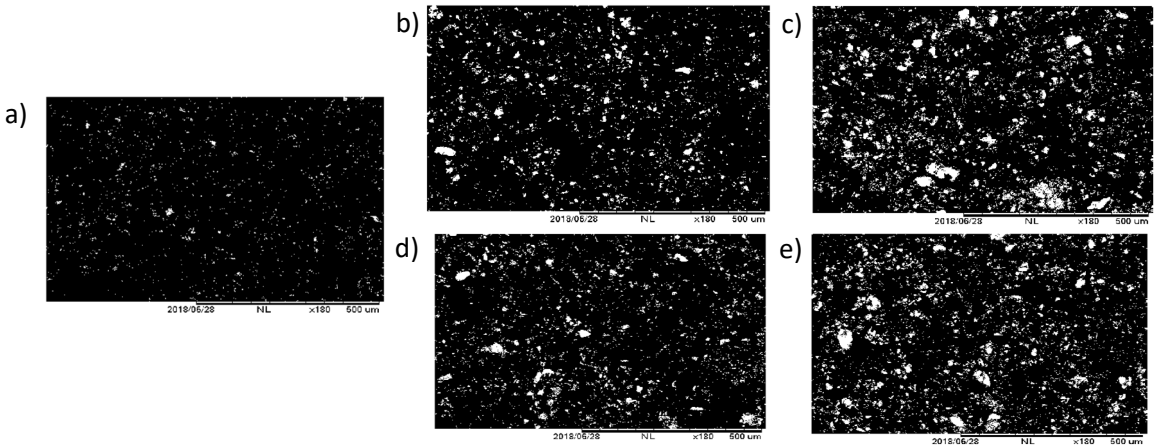

Figure S6. Black and white binary images a) AC, b) ACFeTi5, c) ACFeTi10, d) ACCoTi5 and e) ACCoTi10.

Table S3. Ash content (wt.%) and total number of pixels (TOP) in ¨1¨ binarized SEM images.

Sample	**Ash content (TGA)**	**TOP in ¨1¨ binarized SEM images**	**R^2**
AC	17.19	$2.6*10^4$	
ACFeTi5	22.55	$4.2*10^4$	0.999
ACFeTi10	26.72	$5.6*10^4$	
ACCoTi5	24.15	$4.4*10^4$	0.986
ACCoTi10	29.3	$5.9*10^4$	

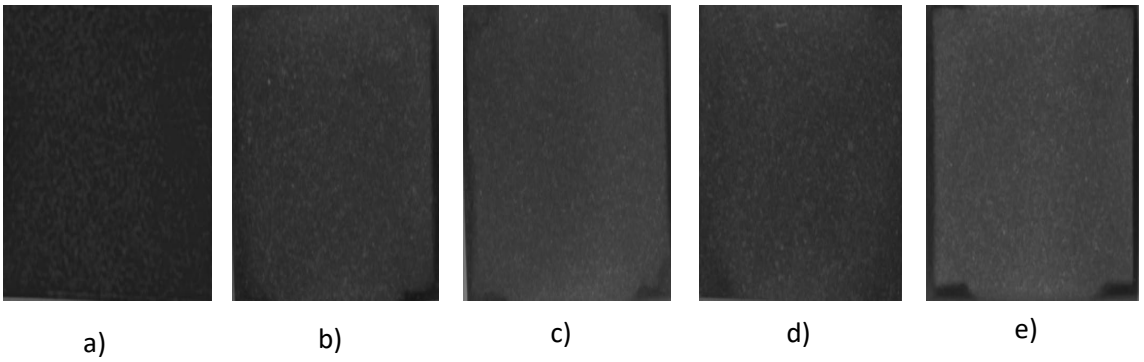

Figure S7. Digital radiographic images of a) AC, b) ACFeTi5, c) ACFeTi10, d) ACCoTi5 and e) ACCoTi10.

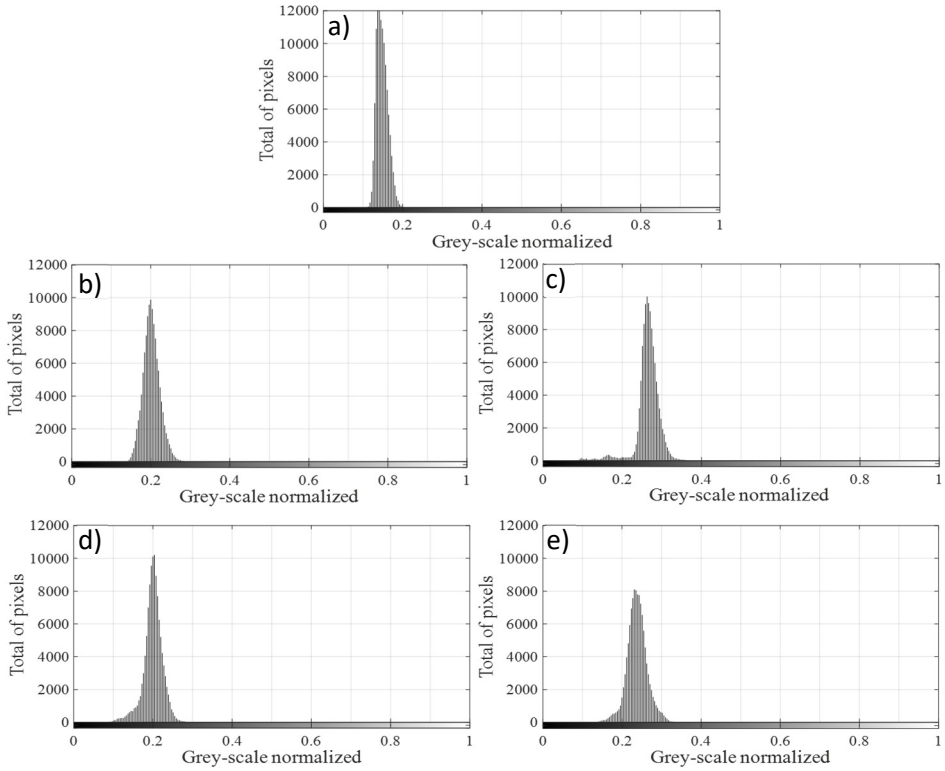

Figure S8. Image histograms of: a) AC, b) ACFeTi5, c) ACFeTi10, d) ACCoTi5 and e) ACCoTi10.

Table S4. Thermally stable inorganic fraction (ash) in wt.(%) and GSI values of attenuated photons.

Sample	**Ash content (TGA)**	**GSI values**	**R^2**
AC	17.19	0.1373	
ACFeTi5	22.55	0.1901	0.999
ACFeTi10	26.72	0.2314	
ACCoTi5	24.15	0.2091	0.986
ACCoTi10	29.3	0.2627	

Table S5. Kinetic parameters for the adsorption of CYF-4G on AC, ACFeTi5, ACFeTi10, ACCoTi5 and ACCoTi10.

Kinetic models	AC	ACFeTi5	ACFeTi10	ACCoTi5	ACCoTi10
q_e, exp. (mg/g)	61.14	50.86	35.36	39.46	26.37
Pseudo-first order (PFO)					
k_1 (1/min)*10^{-2}	1.133	1.281	2.117	1.192	0.924
q_e (mg/g)	69.44	56.67	37.43	47.82	33.65
R^2	0.977	0.961	0.889	0.963	0.983
RMSE	1.884	1.915	1.663	1.782	0.846
Pseudo-second order (PSO)					
k_2 (g/mg min)*10^{-4}	1.941	2.913	8.716	2.725	2.123
q_e(mg/g)	60.37	48.79	34.79	39.45	26.66
R^2	0.986	0.991	0.942	0.991	0.996
RMSE	1.468	0.921	1.205	0.869	0.438
Elovich					
α (mg/g min)	1.909	2.167	6.855	1.046	0.444
β (mg/g)*10^{-2}	6.508	8.657	17.33	8.871	11.35
R^2	0.935	0.879	0.705	0.911	0.959
RMSE	3.191	3.311	2.713	2.757	1.323

Table S6. Kinetic parameters for intraparticle diffusion model.

Weber-Morris	AC	ACCoTi5	ACCoTi10	ACFeTi5	ACFeTi10
Parameters					
First step					
k_{1p} (mg/g $min^{1/2}$)	3.14	2.59	1.55	2.95	2.25
C_1 (mg/g)	9.47	2.51	0.413	4.69	0.323
R^2	0.999	0.999	0.997	0.999	0.996
Second step					
k_{2p} (mg/g $min^{1/2}$)	1.64	0.874	0.852	1.48	0.906
C_2 (mg/g)	29.28	24.85	10.72	25.27	18.67
R^2	0.932	0.998	0.997	0.983	0.883
Third step					
k_{3p} (mg/g $min^{1/2}$)	0.174	0.144	0.264	0.326	0.069
C_3 (mg/g)	54.33	38.25	20.69	43.74	33.58
R^2	0.828	0.773	0.628	0.986	0.928

Table S7. Comparison of the coefficient isotherm parameters for CYF-4G adsorption.

Parameters	AC	ACCoTi5	ACCoTi10	ACFeTi5	ACFeTi10
Q^0_{max} exp. (mg/g)	309.1	244.6	192.2	255.4	203.6
Langmuir					
Q^0_{max} (mg/g)	333.7	246.4	189.2	258.4	201.1
K_L (L/mg)*10^{-2}	5.689	16.64	28.02	6.406	26.82
R^2	0.954	0.944	0.953	0.981	0.933
RMSE	16.84	12.99	7.731	7.549	9.695
Freundlich					
1/n	0.252	0.174	0.152	0.231	0.157
K_F (mg/g)	83.67	66.16	88.91	73.78	92.67
R^2	0.946	0.938	0.914	0.951	0.884
RMSE	18.29	13.57	10.57	11.86	12.72
Temkin					
K_T (L/g)	1.97	13.6	23.1	2.84	16.3
b (kJ/mol)*10^{-2}	1.93	3.07	4.28	2.61	3.83
R^2	0.952	0.836	0.867	0.858	0.879
RMSE	17.22	22.18	13.04	20.15	13.11

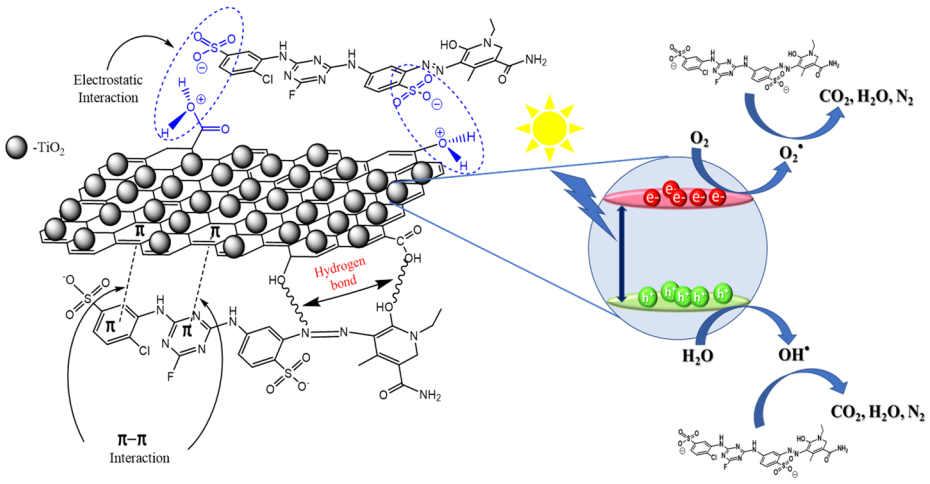

Figure S9. Schematic illustration of visible light photocatalytic degradation mechanism using M-TiO2/AC photocatalyst. M= Co or Fe. [1] after modification.

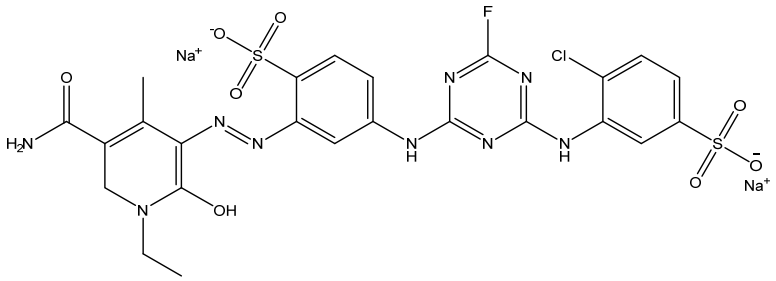

Figure S10. Structure of CYF-4G sodium salt.

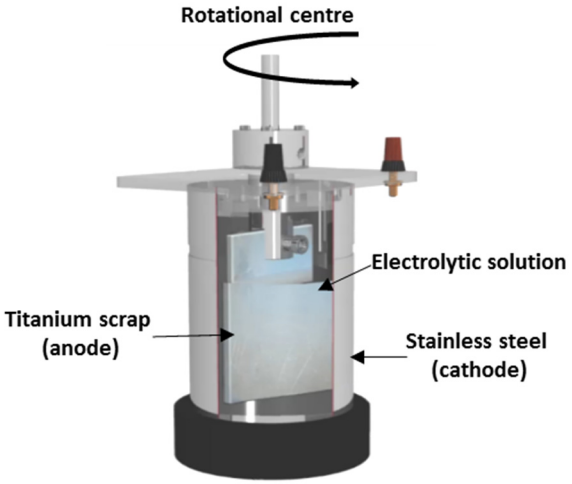

Figure S11. Experimental cell for the electrolytic preparation of nanosized TiO_2.

3. References

1. Machado Garcia, R.; Carleer, R.; Arada Pérez, M.; Gryglewicz, G.; Maggen, J.; Haeldermans, T.; Yperman, J. Adsorption of Cibacron Yellow F-4G dye onto activated carbons obtained from peanut hull and rice husk: kinetics and equilibrium studies. *Biomass Conversion and Biorefinery* **2020**, 1-17, doi:https://doi.org/10.1007/s13399-020-00699-w.